Preoperative Diagnosis of Suprasellar Hemangioblastoma with Four-Dimensional Computed Tomography Angiography: Case Report and Literature Review

Yi Tong[1] Denis Sirhan[2] Maria Cortes[1,3]

[1]Department of Radiology, McGill University Health Center, Montreal, Quebec, Canada
[2]Department of Neurosurgery, Montreal Neurological Hospital and Institute, Montreal, Quebec, Canada
[3]Department of Radiology, Montreal Neurological Hospital and Institute, Montreal, Quebec, Canada

Address for correspondence Maria Cortes, MD, Department of Radiology, Montreal Neurological Hospital and Institute, 3801 University Street, Fifth Floor Radiology, Rm 540A, Montréal, QC H3A 2B4, Canada (e-mail: mariadelpilar.cortes@mcgill.ca).

Indian J Radiol Imaging 2021;31:499–509.

Abstract

Purpose Our case report presents the first case of suprasellar hemangioblastoma diagnosed preoperatively with dynamic computed tomography angiography (four-dimensional [4D] CTA) in a patient without Von Hippel-Lindau (VHL) disease. We illustrate the imaging characteristics of these exceedingly rare tumors and discuss the role of 4D CTA in confirming this diagnosis and guiding surgical management. Finally, we present a literature review of imaging findings, differential diagnosis, management, and prognosis.

Case A 39-year-old woman known for diabetes mellitus type II and dyslipidemia presented with headache, bitemporal hemianopsia, and mild hyperprolactinemia. Initial diagnosis of suprasellar meningioma separate from pituitary gland was revised to definitive diagnosis of suprasellar hemangioblastoma after 4D CTA.

Conclusion Suprasellar hemangioblastomas are extremely rare, often associated to VHL disease. They present as enhancing as suprasellar mass with prominent intra- and peritumoral vascular flow-voids on magnetic resonance imaging. 4D CTA confirms their vascular nature, demonstrates characteristic rapid shunting with feeding arteries, and enlarged draining veins, and is important in guiding surgical management.

Keywords
- 4D CT angiography
- dynamic CT angiography
- hemangioblastoma
- sella turcica

Key Messages

Suprasellar hemangioblastomas present with enhancement and prominent vascular flow-voids on magnetic resonance imaging. Dynamic computed tomography angiography provides key information such as rapid intratumoral shunting, characteristic feeding arteries, and enlarged draining veins, and is important in surgical planning. Total resection is challenging, but when successful, no recurrence has been reported. Radiotherapy is an alternative treatment option.

Introduction

Suprasellar hemangioblastomas are exceedingly rare entities. In fact, hemangioblastomas most commonly arise in the posterior fossa, but are also found in the spinal cord and retina.[1]

published online
July 28, 2021

DOI https://doi.org/10.1055/s-0041-1734335
ISSN 0971-3026

Thieme Medical and Scientific Publishers Private Ltd. A-12, Second Floor, Sector -2, NOIDA -201301, India

Hemangioblastomas are benign and highly vascularized neoplasms of unclear histological origin[1] representing 1 to 2.5% of all primary intracranial neoplasms. Of note, 30% of hemangioblastomas are linked to Von Hippel-Lindau (VHL) disease.[2] In these cases, the patient often has a known family history or personal history of hemangioblastomas or other stigmata.[1]

We present the first case of suprasellar hemangioblastoma diagnosed preoperatively based on four-dimensional computed tomography angiography (4D CTA) in an adult patient without VHL disease.

Case History

A 39-year-old woman, known for diabetes mellitus type II and dyslipidemia, presented with headache for the past few months. Family history was negative. Bitemporal hemianopsia was confirmed on visual field testing, without other focal neurological deficits. Endocrinological profile showed mild hyperprolactinemia (35 ug/L) (►**Table 1**). CT of the chest, abdomen, and pelvis with contrast were unremarkable.

Initial noncontrast CT scan of the head (►**Fig. 1**) showed a solid, heterogeneous suprasellar mass with no cystic component, calcifications, cavernous sinus involvement, or hyperostosis. The mass was seen separate from normal pituitary gland and sella turcica was not enlarged. Based on imaging findings, a diagnosis of suprasellar mass like chiasmal glioma, suprasellar meningioma, or choroid glioma was offered. Magnetic resonance imaging (MRI) was done to further characterize the lesion.

MRI (►**Figs. 2** and **3**), including MR angiography (MRA) and venography (►**Fig. 4**), was limited by motion artifact but revealed a 33 × 25 × 30 mm solid, heterogeneous mass. This lesion was isointense on T1-weighted images and hyperintense on T2-weighted images. Multiple associated hypointense rounded structures were consistent with peritumoral and intratumoral vascular flow-voids (►**Figs. 2A**, **B** and 3A, B). The lesion was avidly enhancing (►**Figs. 2**D and 3C, D). The mass was seen to compress hypothalamus, pituitary infundibulum, and antero-inferior recess of the third ventricle, with associated cerebral edema in the bilateral inferior frontal regions and mesial temporal areas (►**Fig. 2C**). The optic chiasm was clearly separate from the lesion. MRA demonstrated multiple intratumoral and peritumoral hyperintense

Table 1 Endocrinological profile on admission

	Patient's value	Institutional normal range
Prolactin (ug/L)	35.2	3.3–26.7
TSH (mlU/L)	2.00	0.40–4.40
Thyroxine (free) (pmol/L)	8.20	8.00–18.00
LH (IU/L)	0.3	N/A
FSH (IU/L)	0.6	N/A
GH (ug/L)	0.10	0.03–4.00
ACTH (pmol/L)	3.32	1.60–13.90
Cortisol AM (nmol/L)	221	120–535
Cortisol random (nmol/L)	178	120–535

Abbreviations: ACTH, adrenocorticotropic hormone; FSH, follicle-stimulating hormone; GH, growth hormone; LH, luteinizing hormone; TSH, thyroid stimulating hormone.

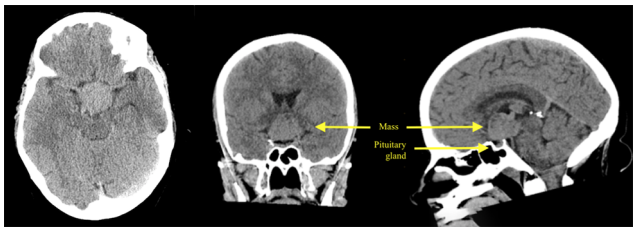

Fig. 1 Initial computed tomography (CT) head (noncontrast).

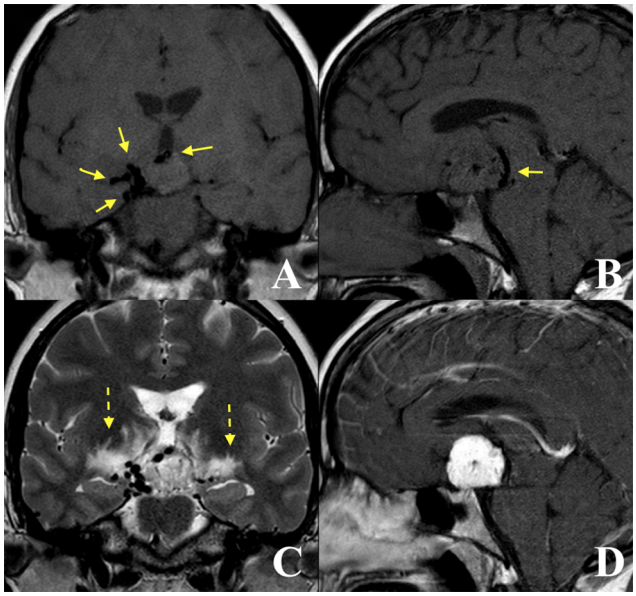

Fig. 2 Magnetic resonance imaging.

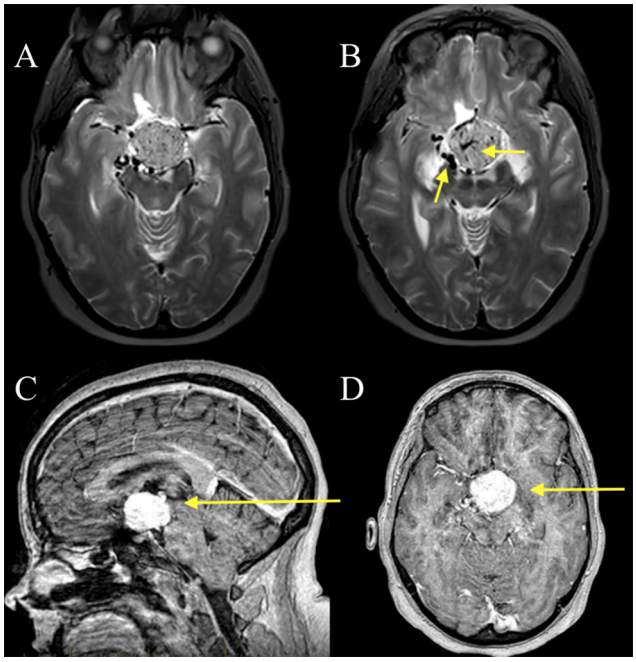

Fig. 3 Magnetic resonance imaging.

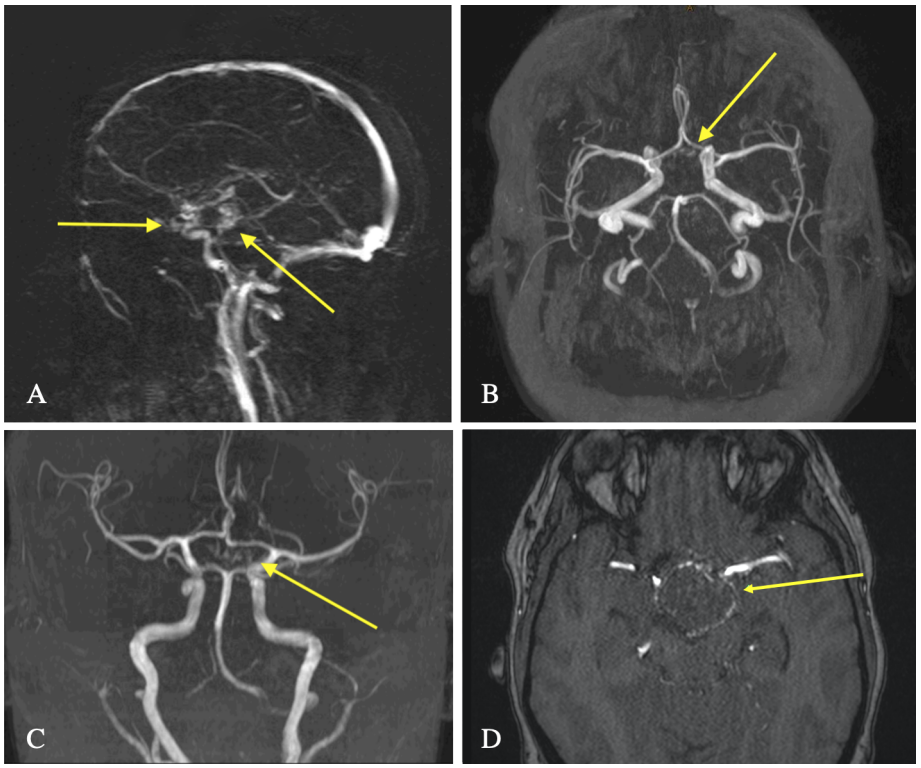

Fig. 4 Magnetic resonance angiography.

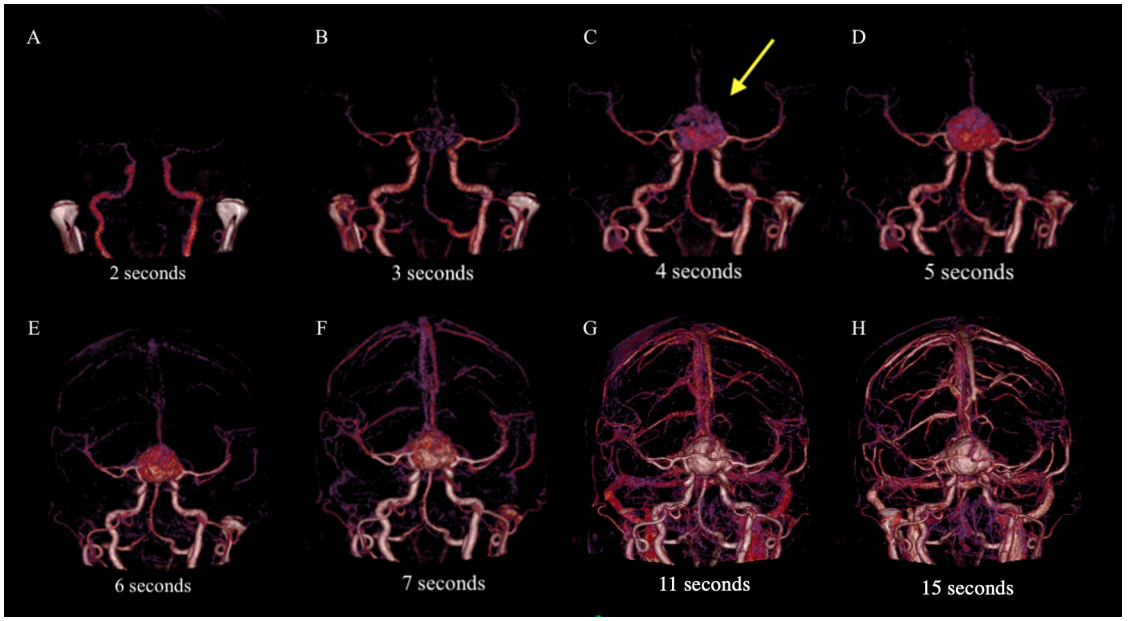

Fig. 5 CTA 4D images demonstrating arterial to venous phases with early contrast opacification of the suprasellar tumor.

curvilinear structures, consistent with high tumoral vascularity, without evidence of aneurysm or arteriovenous malformation (►**Fig. 4**).

In light of the findings on CT and MRI, a few differential diagnoses were considered, notably papillary subtype of craniopharyngioma, chiasmal-hypothalamic glioma, and meningioma arising from the dorsum sellae (see the "Discussion" section).

Due to atypical appearance on MRI and to better characterize the surrounding vasculature (notably the prominent draining veins) in prevision of a surgical intervention, the patient underwent dynamic CTA (4D CTA) (see **Appendix A**, "Materials and Methods" for technical details) which showed marked curvilinear enhancement around the mass, reflecting a combination of large feeding arteries and prominent venous drainage (►**Fig. 5**). The appearance suggested

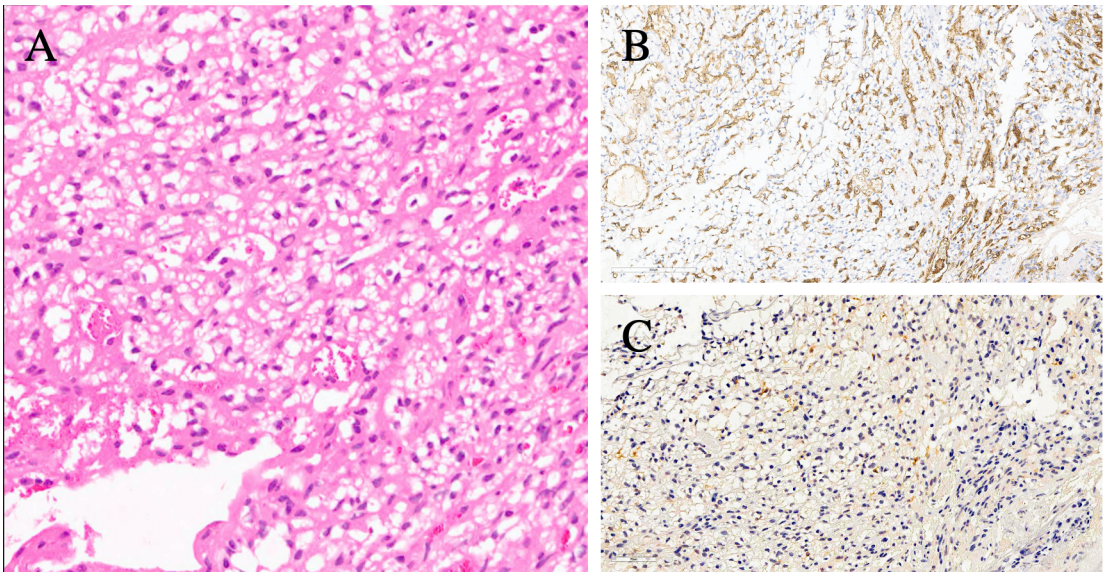

Fig. 6 Histopathology slides of the tumor. (A) H&E stain showing a highly vascular tumor with thin walled capilaries. (B) Immunohistochemistry stain with CD34. (C) Inhibin stain positive confirmeing the diagnosis of hemangioblastoma.

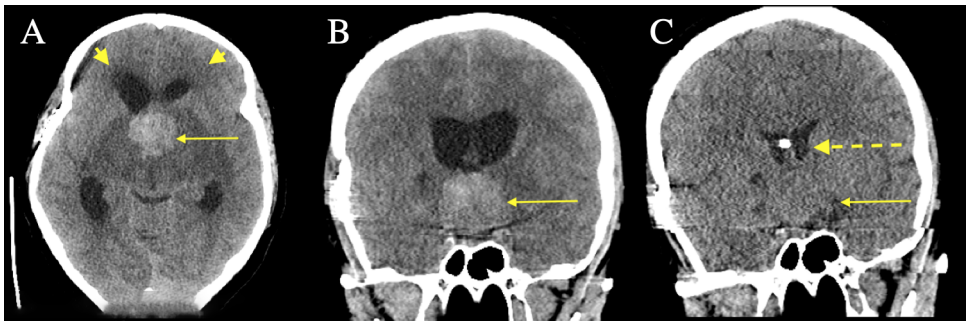

Fig. 7 CT Images of the brain, 9 months post operative, demonstrating intratumoral spontaneous bleeding and hydrocephalus.

very rapid intratumorally shunting, as one classically sees on angiographical studies of typical posterior fossa hemangioblastomas.

After 4D CTA, the report was revised to consider suprasellar hemangioblastoma as the most likely diagnosis and this was communicated to the neurosurgical team. The patient underwent right pterional and subfrontal craniotomy for tissue sampling and possible resection. Intraoperatively, the tumor was noted to be purple and vascular-appearing, adjacent to a highly prefixed chiasm. A biopsy of the tumor was taken. Given the intraoperative findings and preoperative radiological characteristics, all suggestive of high risk of hemorrhage, no resection was attempted. There were no intraoperative complications.

Immunohistochemistry confirmed the diagnosis of hemangioblastoma with focal positive staining for inhibin (►**Fig. 6**). The patient underwent stereotaxic radiosurgery 4 months after her operation. Unfortunately, her treatment was complicated by panhypopituitarism, leading to adrenal crisis.

Nine months after her craniotomy and biopsy, the patient presented with sudden onset of headache and vomiting. On nonenhanced CT (►**Fig. 7**), findings were suggestive of acute rebleeding of the suprasellar hemangioblastoma with mass effect on the basal cisterns, as well as suspected intraventricular extension of the hemorrhage. There was associated findings of acute communicating hydrocephalus (►**Fig. 7**), possibly secondary to the acute mass effect or due to intraventricular hemorrhagic components. The patient was treated with ventriculoperitoneal shunt placement. After further treatment with stereotaxic radiosurgery, the tumor minimally reduced in size (►**Fig. 7**). At her last follow-up appointment, 12 months after her initial presentation, the patient was medically stable. Unfortunately, she was subsequently lost to follow-up.

Discussion

In the past 40 years, 33 cases of suprasellar hemangioblastomas have been reported in live patients (►**Table 2**): 19 of these cases have been patients with VHL and 12 cases of patients without VHL, with two cases of unclear VHL status. Overall, 30% of hemangioblastomas are associated with VHL, but a sellar or suprasellar location seems to have a stronger association to the disease.[2,3] Our patient's symptoms were congruent with the most commonly reported symptoms ("visual disturbances" and "headache") (►**Table 2**).

Table 2 Reported cases of suprasellar hemangioblastoma in the literature

	Patient	Presentation	VHL	Imaging	Preop Dx	Treatment	Follow-up	Year, Ref
1	19M	Vertigo, vomiting, ataxia, nystagmus	+	CT: enhancing solid nodule on the right anterior edge of the suprasellar cistern Angio: supraclinoid nodule	N/A	Craniotomy (total excision) Sacrifice of optic nerve	N/A	1981[4]
2	28F	Headache, amenorrhea, galactorrhea	–	CT: enhancing solid Angio: highly vascularized with persistent blush	Meningioma	Right frontal craniotomy (total excision)	Alive at 2 mo (panhypopit)	1984[5]
3	60F	Partial hemianopsia	+	CT: 24 mm suprasellar solid mass	HBL	Radiosurgery	Alive at 28 mo, SIADH, tumor reduced by 54%	1996[6]
4	20F	Secondary amenorrhea, polydipsia	+	MRI: 6-mm contrast-enhancing mass of the tuber cinereum, immediately posterior to optic chiasm and two enhancing masses in right cerebellar hemisphere	HBL	Modified transsphenoidal approach	No residual tumor at 53 mo (panhypopit and DI)	2000[7]
5	15F	Asymptomatic	+	MRI: 7 × 14mm enhancing lesion compressing left optic nerve and 1 cm enhancing in vermis	HBL	Modified transsphenoidal approach	No residual tumor at 12 mo (CSF leak POD #6)	2000[7]
6	33F	Menses irregularity. Mildly abnormal GnRH stimulation test	+	MRI: 8 mm round, homogeneous enhancement, T1 isointense, T2 cystic Angio: tumor blush fed by superior hypophyseal artery	HBL	Right frontotemporal craniotomy	No residual tumor at 6 mo	2001[8]
7	62M	Visual disturbances	–	Angio: "remarkable tumor staining" originating from the right and left ICA and the left ECA MRI: homogeneous enhancement, T2 hyperintense	Meningioma	Craniotomy	Paraparesis POD #7	2001[9]
8	40F	Oligomenorrhea, memory lapses	+	MR: 3.2 cm solid, homogeneous enhancement T1 isointense, T2 heterogeneous (hyper/iso), intratumoral flow-void Angio: hypervascular mass, fed by small perforators from distal ICA and thalamoperforating arteries	HBL (previous cerebellar)	Subtotal excision + radiosurgery	N/A	2003[10]
9	54M	Temporal hemianopsia left + complete visual loss right	–	MRI: Homogeneous marked enhancement T1 Isointense, T2 hyperintense	Meningioma	Right pterional craniotomy	No residual tumor at 5 y	2004[11]
10	38M	Complete visual loss (left eye), severe headaches	+	MRI: Homogeneous enhancement T1 Isointense, T2 hyperintense	HBL (previous cerebellar)	Right pterional craniotomy (subtotal)	N/A	2004[11]

(*Continued*)

Table 2 (*Continued*)

	Patient	Presentation	VHL	Imaging	Preop Dx	Treatment	Follow-up	Year, Ref
11	51F	Progressive right inferior temporal quadranopsia	+	MRI: 20 mm diameter, T1 isointense homogenous, T2 hyperintense, strong contrast enhancement	HBL (previous retinal and spinal HBL)	Left frontopterional craniotomy	8-year follow-up: panhypopit, no pituitary recurrence, 5 new cerebellar HBLs (RadioTx)	2007[12]
12	59F	Fatigue, decreased vision, somnolence, impaired memory	?	Angio: blush from both superior hypophyseal arteries MRI: 3.5-cm enhancing lesion, small cystic structures, T1 isointense, T2 hyperintense	N/A	Bifrontal interhemispheric craniotomy	No residual tumor at 3 y (panhypopit)	2008[13]
13–20	38 ± 13 y, 4 female4 male	Asymptomatic, normal endocrine profile, normal visual testing	+	MRI: mean tumor volume 0.5 ± 0.9 cm^3	N/A	Observation	Mean follow-up 41.4 ± 14.4 mo, no deficits	2009[14]
21	30M	Progressive vision loss	+	No details provided	N/A	Craniotomy but no attempt at resection	Death at 120 mo (cause directly linked to HBL)	2010[15]
22	28F	27-mo history of galactorrhea and alopecia	+	MRI: 4 × 2 × 2mm pituitary infundibulum mass with rapid contrast enhancement	HBL (previous spinal and cerebellar HBLs resected)	Bromocriptine	Galactorrhea resolved after 2 wk of bromocriptine	2010[16]
23	80F	Episode of severe headache with nausea, vomiting, and blurred vision (pituitary apoplexy). Known 12-year history of stable sellar mass	–	MRI: acute hemorrhage of sellar mass	Pituitary adenoma	Transnasal, transsphenoidal total resection	Panhypopit with transient DI. No recurrence at 16 mo	2011[17]
24	12F	Headache and bitemporal hemianopsia, hypopituitarism	–	MRI: homogeneous contrast enhancement and optic chiasm compression, intratumoral and peritumoral engorged vessels	Pituitary adenoma	2 attempts (transsphenoidal and transcranial), stopped for bleeding	Clinically improved at 3 mo	2012[18]
25	64F	Headache, bitemporal hemianopsia Normal endo	–	CT: solid suprasellar mass of 2.5 cm diameter MRI: T1 isointense, T2 hyperintense, curvilinear areas of flow-void, strong enhancement, with cystic component CT angio: supplied by multiple small perforating arteries from ACA and PCom	Craniopharyngioma	Endoscopic endonasal subtotal resection	1 mo postop: subtotal resection. CSF leak and hydrocephalus (VP shunt)	2013[19]
26	60F	Headache, dizziness	–	MRI: T1 isointense, T2 heterogeneous, multiple signal voids inside mass, marked homogeneous contrast enhancement	N/A	Right frontotemporal craniotomy	Transient DI, no neuro or endo deficits at 1 y	2015[20]

(*Continued*)

Table 2 (*Continued*)

	Patient	Presentation	VHL	Imaging	Preop Dx	Treatment	Follow-up	Year, Ref
27	51F	Headache, left visual field defect	–	MRI: solid mass, T1 isointense, T2 hyperintense with homogeneous contrast enhancement	N/A	Left pterional craniotomy	No residual at 1 y (transient DI)	2015[2]
28	35F	Neurofibromatosis 1, headache, near complete visual loss right eye	–	MRI: 8 mm lesion with small cystic components, T1 isointense, T2 hyperintense, marked contrast enhancement		Endoscopic expanded transsphenoidal resection with sphenoidectomy	Transient DI (lasting 4 mo), stable 11 mo postop	2016[21]
29	67F	Retro-orbital pain, bilateral upper temporal quadrantanopsia, mild DI	–	MRI: Significant enhancement, slight upward displacement of optic chiasm	N/A	Transsphenoidal resection	DI	2017[22]
30	64F	Left inferior quadrantanopsia, (right eye enucleated)	+	MRI: T1 avid enhancement, no other details reported	N/A	Octreotide intramuscular (unresectable)	~25% decrease in tumor volume after 9 mo	2017[23]
31	38F	9 mo history of amenorrhea with low LH and FSH, headaches	?	MRI: 13 × 13 × 13.2 mm mass in upper half of infundibulum, T1 isointense, T2 isointense, avid contrast enhancement, unremarkable on DWI and ADC map	Pituicytoma	Endoscopic transsphenoidal total resection	N/A	2017[24]
32	60F	Headache, abducens palsy, low ATCH	–	MRI: 14 × 12 mm, rounded mass attached to the pituitary stalk, avidly enhancing, multiple flow-voids, fed by short perforators from the left ICA and posterior communicating artery	HBL	Right OZ craniotomy	Stable at 36 mo, improved vision and endocrine function	2018[25]
33	28F	Bitemporal hemianopsia	–	CT: no calcification MRI: 10 × 7 × 12 mm solid tumor with accompanying 10 mm cystic component, T1 isointense T2 hyperintense, avidly enhancing, edema-like change along the optic tract	Craniopharyngioma	Biopsy attempt (excess bleed > 1 L) then complete excision	No tumor recurrence at 6 mo	2018[26]

Abbreviations: ACA, anterior cerebral artery; ACTH, adrenocorticotropic hormone; ADC, apparent diffusion coefficient; CSF, cerebrospinal fluid; CT, computed tomography; DI, diabetes insipidus; DWI, diffusion-weighted imaging; Dx, diagnosis; ECA, external carotid artery; FSH, follicle-stimulating hormone; GnRH, gonadotropin releasing hormone; HBL, hemangioblastoma; ICA, internal carotid artery; LH, luteinizing hormone; MRI, magnetic resonance imaging; OZ, orbitozygomatic; panhypopit, panhypopituitarism; PCom, posterior communicating artery; POD, postop day; SIADH, syndrome of inappropriate antidiuretic hormone; VHL, Von Hippel-Lindau; VP, ventriculoperitoneal.

This case is the first reported preoperatively diagnosed suprasellar hemangioblastoma confirmed on 4D CTA in a patient with no evidence of VHL disease. In such sporadic cases, previous reports describe preoperative diagnoses like craniopharyngioma, pituitary adenoma, pituicytoma, and meningioma.[5,9,11,13,18,19,26] Our case's unusual imaging features prompt consideration of less frequent suprasellar tumors like papillary craniopharyngioma, angiomatous meningioma, hemangiopericytoma, as well as chordoid glioma.

The rare papillary subtype represents about one-third of adult craniopharyngiomas. These lesions are predominantly solid or mixed solid-cystic and have a predilection to involve the third ventricle. Notably, papillary craniopharyngiomas do not contain calcifications. On MRI, the usual appearance is hypointense on T1-weighted images, hyperintense on T2-weighted images, with cyst wall enhancement postgadolinium.[27,28] In our case, papillary subtype of craniopharyngioma was considered in the differential but the

significant presence of intratumoral and peritumoral vascular flow-voids was deemed atypical.

As for angiomatous meningioma, a very rare histological subtype of meningiomas, they have a male predominance. These dural-based lesions can arise from the skull base, with high attenuation on CT. The angiomatous histological type appears hypointense on T1-weighted images, hyperintense on T2-weighted images, and hypointense on diffusion-weighted imaging. Due to prominent hypervascularity, it enhances avidly with internal vascular flow-voids and surrounding brain edema. Other features may be present, such as a dural tail, involvement or encasement of the cavernous internal carotid artery, and bone erosion.[29,30] In our case, the diagnosis of a highly vascular meningioma was entertained, given the location and MRI appearance. However, there was notable absence of associated findings such as a dural tail, internal carotid artery involvement, or bone erosion.

Another uncommon lesion to consider would be hemangiopericytoma, a tumor that tends to be large and lobulated in appearance, with intense but heterogeneous enhancement. It rarely shows calcifications but is frequently associated with peritumoral edema.[31-33] Up to 20% of cases have malignant behavior, with possible metastasis outside of the central nervous system (bone, liver, lungs).[31,32] On MRI, hemangiopericytomas are usually isointense with heterogeneous contrast enhancement[31,32] and prominent internal signal voids.[32] A dural tail is seen in approximately 50% of cases.[31] More than half of cases have bone erosion.[32] The lesion of our presented case did not have a dural tail and lacked aggressive features such as bone erosion. Our patient had no evidence of metastatic lesions on MRI of the head and CT of the chest, abdomen, and pelvis.

Finally, a differential diagnosis for lesions near the third ventricle includes chordoid gliomas, which predominantly occur in adult women. On MRI, this tumor shows a well-defined ovoid mass in the anterior third ventricle or sellar region. It is isointense on T1-weighted images with uniform contrast enhancement and bilateral vasogenic edema. On CT, it is hyperdense to gray matter.[34] However, a main feature of the tumor in our case is the presence of prominent vascular flow-voids, which is not typical for chordoid gliomas.

Thus, the preoperative diagnosis of suprasellar hemangioblastoma is challenging due to its rarity and the many other entities to be considered in the differential, as detailed above. Our case presents typical MRI features of hemangioblastomas: isointense on T1-weighted images, hyperintense on T2-weighted images, with marked contrast enhancement (►**Table 2**). These lesions can also have a cystic appearance, but surrounding edema, as in our case, is more atypical. Most importantly, hemangioblastomas have prominent vascular flow-voids on MRI.

Although MRI and MRA provide high-quality visualization of the intracranial arteries, the appearance of vascular lesions is influenced by size, flow direction, pulsatility, flow velocity, and degree of thrombosis.[35-38] 4D CTA is known to have excellent spatial and temporal resolution and is uniquely helpful in evaluating structures of the skull base.[35,36] In addition, 4D CTA is reported to have a better sensitivity than MRA with better visualization of surrounding vessel anatomy and is less prone to flow-related or motion artifacts.[36] Moreover, in our case, 4D CTA was essential in evaluating venous drainage, and in general, is very helpful in planning interventions on complex skull base tumors.[36] 4D CTA is a less invasive modality than traditional angiography (digital subtraction angiography [DSA]), with near-equal sensitivity and specificity in the evaluation of aneurysms,[37] but DSA remains the gold standard when evaluating vascular neoplasms of the head and neck.

For a hemangioblastoma, 4D CTA will clearly demonstrate characteristic features of very rapid shunting, large feeding arteries with dilated draining veins, and a deep tumor blush. The early venous shunting confirmed rapid flow within the tumor, and also helped for the surgical planning. In terms of differential diagnosis, the appearance of meningioma on 4D CTA is different, typically featuring a persistent tumor blush with delayed washout, in contrast with the early venous drainage of hemangioblastoma.[39] Moreover, a meningioma classically features a central vascular pedicle from which smaller vessels radiate ("spoke wheel" appearance) and often features vascular supply from prominent meningeal or pial vessels.[39] The high-resolution dynamic characteristics of 4D CTA provide added diagnostic benefit compared with MRI and MRA. In our case, 4D CTA was deemed to have provided adequate quality of dynamic diagnostic information and DSA was not performed. Of note, 4D contrast-enhanced MRA is another imaging modality that can provide reliable hemodynamic diagnostic information in head and neck tumors. Even though 4D contrast-enhanced MRA is useful in characterizing tumor stain, this modality is not a replacement to DSA due to poorer temporal resolution (more specifically, poorer identification of feeding arteries).[40]

Preoperative diagnosis of hemangioblastoma is important for surgical management. Resection of suprasellar hemangioblastomas is often limited by surrounding structures[4] and risk of hemorrhage.[18,26] In all cases of successful total resection, the tumor did not recur.[2,7,8,11,13,26] However, important surgical complications include cerebrospinal fluid leak,[7,19] hydrocephalus,[19] and paraparesis.[9] Postoperative endocrine dysfunction can include panhypopituitarism,[5,8,35] diabetes insipidus,[2,6] and syndrome of inappropriate antidiuretic hormone.[6] The option of preoperative embolization is mitigated by risks of infarct.[41] Targeted radiotherapy has shown good results in tumor volume reduction.[7,42] Intramuscular octreotide in a small group of VHL patients with hemangioblastomas expressing somatostatin receptors has also been linked to significant tumor volume reduction; however, this remains experimental.[23]

Conclusion

Suprasellar hemangioblastoma is an extremely rare diagnosis and presents as a mass with prominent vascular flow-voids on MRI. 4D CTA can confirm the vascular nature of the lesion and characteristic features of very rapid shunting, large feeding arteries, dilated draining veins, and deep tumor blush.

Dynamic imaging also helps in guiding the surgical approach and can influence intraoperative decisions. A hemangioblastoma located in the sellar-suprasellar region is often associated to VHL disease. Surgical resection is complex due to tumor location. Benefits must be weighed against the high risk of hemorrhage and other postoperative complications. However, there are no reported cases of recurrence after total resection. Treatment with radiotherapy is another option.

Presentation at a Meeting
American Society of Neuroradiology 2019 Annual Meeting, Boston, MA, USA, May 20th, 2019.

Source(s) of Support
None to declare.

Conflict of Interest
None declared.

Acknowledgments
None.

References

1 Metelo A, Iliopoulos O, Hemangioblastomas of the Central Nervous System. In: Rosenberg RN, Pascual JM, eds. Rosenberg's Molecular and Genetic Basis of Neurological and Psychiatric Disease. 5th ed. London: Academic Press; 2015 955–961
2 Li Z, Feng T, Teng H, Hu Y, Yao Y, Liu Y. Suprasellar hemangioblastoma without von Hippel-Lindau disease: a case report and literature review. Int J Clin Exp Pathol 2015;8(6):7553–7558
3 Mills SA, Oh MC, Rutkowski MJ, Sughrue ME, Barani IJ, Parsa AT. Supratentorial hemangioblastoma: clinical features, prognosis, and predictive value of location for von Hippel-Lindau disease. Neuro-oncol 2012;14(8):1097–1104
4 O'Reilly GV, Rumbaugh CL, Bowens M, Kido DK, Naheedy MH. Supratentorial haemangioblastoma: the diagnostic roles of computed tomography and angiography. Clin Radiol 1981;32(4):389–392
5 Grisoli F, Gambarelli D, Raybaud C, Guibout M, Leclercq T. Suprasellar hemangioblastoma. Surg Neurol 1984;22(3):257–262
6 Niemelä M, Lim YJ, Söderman M, Jääskeläinen J, Lindquist C. Gamma knife radiosurgery in 11 hemangioblastomas. J Neurosurg 1996;85(4):591–596
7 Kouri J, Chen MY, Watson JC, Oldfield EH. Resection of suprasellar tumors by using a modified transsphenoidal approach. Report of four cases. J Neurosurg 2000;92(6):1028–1035
8 Goto T, Nishi T, Kunitoku N, et al. Suprasellar hemangioblastoma in a patient with von Hippel-Lindau disease confirmed by germline mutation study: case report and review of the literature. Surg Neurol 2001;56(1):22–26
9 Ikeda M, Asada M, Yamashita H, Ishikawa A, Tamaki N. A case of suprasellar hemangioblastoma with thoracic meningioma [in Japanese]. No Shinkei Geka 2001;29(7):679–683
10 Wasenko JJ, Rodziewicz GS. Suprasellar hemangioblastoma in Von Hippel-Lindau disease: a case report. Clin Imaging 2003;27(1):18–22
11 Peker S, Kurtkaya-Yapicier O, Sun I. Sav A, Pamir MN. Suprasellar haemangioblastoma. Report of two cases and review of the literature. J Clin Neurosci 2005;12(1):85–89
12 Fomekong E, Hernalsteen D, Godfraind C, D'Haens J, Raftopoulos C. Pituitary stalk hemangioblastoma: the fourth case report and review of the literature. Clin Neurol Neurosurg 2007;109(3):292–298
13 Miyata S, Mikami T, Minamida Y, Akiyama Y, Houkin K. Suprasellar hemangioblastoma. J Neuroophthalmol 2008;28(4):325–326
14 Lonser RR, Butman JA, Kiringoda R, Song D, Oldfield EH. Pituitary stalk hemangioblastomas in von Hippel-Lindau disease. J Neurosurg 2009;110(2):350–353
15 Peyre M, David P, Van Effenterre R, et al. French NCI Network VHL Disease and Inherited Predisposition to Kidney Cancer. Natural history of supratentorial hemangioblastomas in von Hippel-Lindau disease. Neurosurgery 2010;67(3):577–587, discussion 587
16 Cao Y, Gao P, Wang S, Zhao J. Pituitary infundibulum hemangioblastoma detected by dynamic enhancement MRI. Can J Neurol Sci 2010;37(5):697–699
17 Schär RT, Vajtai I, Sahli R, Seiler RW. Manifestation of a sellar hemangioblastoma due to pituitary apoplexy: a case report. J Med Case Reports 2011;5(496):496
18 Ajler P, Goldschmidt E, Bendersky D, et al. Sellar hemangioblastoma mimicking a macroadenoma. Acta Neurol Taiwan 2012;21(4):176–179
19 Xie T, Zhang X, Hu F, et al. Suprasellar hemangioblastoma mimicking a craniopharyngioma: result of extended endoscopic transsphenoidal approach–case report. Neurol Med Chir (Tokyo 2013;53(10):735–739
20 Lee GI, Kim JM, Choi KS, Kim CH. Sporadic hemangioblastoma in the pituitary stalk: a case report and review of the literature. J Korean Neurosurg Soc 2015;57(6):465–468
21 Kosty J, Staarman B, Zimmer LA, Zuccarello M. Infundibular hemangioblastoma in a patient with neurofibromatosis type 1: case report and review of the literature. World Neurosurg 2016;88:693.e7–693.e12
22 Wenting J, Ogawa Y, Ito J, Tominaga T. Suprasellar hemangioblastoma unrelated to von Hippel-Lindau disease successfully treated through extended transsphenoidal approach: diagnostic value of Von Hippel-Lindau disease gene-derived protein. J Neurol Surg A Cent Eur Neurosurg 2017;78(3):296–301
23 Sizdahkhani S, Feldman MJ, Piazza MG, et al. Somatostatin receptor expression on von Hippel-Lindau-associated hemangioblastomas offers novel therapeutic target. Sci Rep 2017;7:40822
24 Pakdaman MN, Austin MJ, Bannykh S, Pressman BD. Sporadic hemangioblastoma arising from the infundibulum. J Radiol Case Rep 2017;11(5):1–6
25 Alshafai N, Maduri R, Shail M, Chirchiglia D, Meyronet D, Signorelli F. Surgical approach for suprasellar hemangioblastomas preserving the pituitary stalk: review of the literature and report of a further case. Clin Neurol Neurosurg 2018;168:147–152
26 Hattori Y, Tahara S, Yamada O, Yamaguchi M, Ishisaka E, Morita A. Suprasellar hemangioblastoma with reversible edema-like change along the optic tract: a case report and literature review. World Neurosurg 2018;114:187–193
27 Zada G, Lopes MBS, Mukundan S Jr, Laws E Jr, Craniopharyngiomas. In: Zada G, Lopes MBS, Mukundan Jr. S, Laws Jr. E, eds. Atlas of Sellar and Parasellar Lesions. Cham: Springer International Publishing Switzerland; 2016 197–210
28 Crotty TB, Scheithauer BW, Young WF Jr, et al. Papillary craniopharyngioma: a clinicopathological study of 48 cases. J Neurosurg 1995;83(2):206–214
29 Zada G, Lopes MBS, Mukundan S Jr, Laws E Jr, Meningioma of the sellar and parasellar region. In: Zada G, Lopes MBS, Mukundan Jr. S, Laws Jr. E, eds. Atlas of Sellar and Parasellar Lesions. Cham: Springer International Publishing Switzerland; 2016 259–270
30 Kunimatsu A, Kunimatsu N, Kamiya K, Katsura M, Mori H, Ohtomo K. Variants of meningiomas: a review of imaging findings and clinical features. Jpn J Radiol 2016;34(7):459–469

31 Zada G, Lopes MBS, Mukundan S Jr, Laws E Jr, Hemangiopericytoma. In: Zada G, Lopes MBS, Mukundan Jr. S, Laws Jr. E, eds. Atlas of Sellar and Parasellar Lesions. Cham: Springer International Publishing Switzerland; 2016 271–274
32 Han MH, Cho YD, Kim YD, Kin DH. Recurrent sellar and suprasellar hemangiopericytoma. J Korean Neurosurg Soc 2007;41:425–428
33 Jalali R, Srinivas C, Nadkarni TD, Rajasekharan P. Suprasellar haemangiopericytoma–challenges in diagnosis and treatment. Acta Neurochir (Wien 2008;150(1):67–71
34 Pomper MG, Passe TJ, Burger PC, Scheithauer BW, Brat DJ. Chordoid glioma: a neoplasm unique to the hypothalamus and anterior third ventricle. AJNR Am J Neuroradiol 2001;22(3):464–469
35 Gupta S, Bi WL, Mukundan S, Al-Mefty O, Dunn IF. Clinical applications of dynamic CT angiography for intracranial lesions. Acta Neurochir (Wien 2018;160(4):675–680
36 Bi WL, Brown PA, Abolfotoh M. Al-Mefty O, Mukundan S Jr, Dunn IF. Utility of dynamic computed tomography angiography in the preoperative evaluation of skull base tumors. J Neurosurg 2015;123(1):1–8
37 Villablanca JP, Jahan R, Hooshi P, et al. Detection and characterization of very small cerebral aneurysms by using 2D and 3D helical CT angiography. AJNR Am J Neuroradiol 2002;23(7):1187–1198
38 Takhtani D, Dundamadappa S, Puri AS, Wakhloo A. Flow artifact in the anterior communicating artery resembling aneurysm on the time of flight MR angiogram. Acta Radiol 2014;55(10):1253–1257
39 Huang RY, Bi WL, Griffith B, et al; International Consortium on Meningiomas. Imaging and diagnostic advances for intracranial meningiomas. Neuro-oncol 2019;21(Suppl 1) :i44–i61
40 Nishimura S, Hirai T, Shigematsu Y, et al. Evaluation of brain and head and neck tumors with 4D contrast-enhanced MR angiography at 3T. AJNR Am J Neuroradiol 2012;33(3):445–448
41 Ene CI, Xu D, Morton RP, et al. Safety and efficacy of preoperative embolization of intracranial hemangioblastomas. Oper Neurosurg (Hagerstown 2016;12(2):135–140
42 Sawin PD, Follett KA, Wen BC. Laws ER Jr. Symptomatic intrasellar hemangioblastoma in a child treated with subtotal resection and adjuvant radiosurgery. Case report. J Neurosurg 1996;84(6):1046–1050

Appendix A: Materials and Methods

The computed tomography angiography (CTA) was obtained using a Toshiba Aquilion One 320-slice multidetector computed tomography scanner. As per protocol, 50 mL of Isovue (iopamidol 300 mg/mL of iodine; Bracco Diagnostics Inc., Monroe Township, New Jersey, United States) contrast material was infused. A total of 24 sequential volumes covering the entire brain were acquired at 0.5 mm thickness that covers 16 cm of the head in a *z* plane. The protocol includes a series of intermittent volume scans over a period of 60 seconds. The first volume is used as the mask for the dynamic subtraction. A series of low-dose scans are obtained, first for every 2 seconds during the arterial phase, and then are spaced out to every 5 seconds to capture the slower venous flow. The mA exposure is increased during the peak arterial enhancement to provide superior three-dimensional (3D) images of the intracranial arteries for a maximum of 310 mA (kV 80). The raw data are reconstructed into a dynamic volume imaging to provide a true four-dimensional computed tomography angiography (4D CTA) and digital subtraction angiography (DSA) image of the intracranial circulation.

